Analyst

Cite this: *Analyst*, 2011, **136**, 4809

www.rsc.org/analyst

PAPER

Design of a dual-signaling sensing system for fluorescent ratiometric detection of Al^{3+} ion based on the inner-filter effect†

Yongxiang Wang, Limin Xiong, Fenghua Geng, Fuqiang Zhang and Maotian Xu*

Received 8th July 2011, Accepted 22nd August 2011
DOI: 10.1039/c1an15566k

A dual-signal sensing system based on the inner-filter effect (IFE) was demonstrated, in which the combination of two signaling mechanisms allows metal binding to turn on two fluorescence emission bands, independently. A proof-of-concept fluorescent ratiometric assay for Al^{3+} in pure aqueous solution is presented. The proposed assay is based on the Al^{3+}-induced color and fluorescence changes of Alizarin red S (ARS) and IFE between ARS and *meso*-tetra(*N*-methyl-4-pyridyl)porphine tetratosylate salt (TMPyP). In the absence of Al^{3+}, the absorption spectrum of the ARS in 0.2 M HAc–NaAc buffer (pH 5.5) has a strong peak at 420 nm, significantly overlapping with the excitation of TMPyP. ARS is expected to be capable of functioning as a powerful absorber to tune the emission of TMPyP on account of the spectral overlap. Binding of Al^{3+} with ARS forms a fluorometric ARS/Al^{3+} complex and shifts the maximum absorbance from 420 nm to 480 nm, which overlaps negligibly with the excitation of TMPyP and turns on the proper emission spectrum for TMPyP. Under the optimum conditions, The fluorescence intensity ratio, F_{585}/F_{651}, responds to Al^{3+} over a dynamic range of 0.1–1.5 μM, with a limit of detection of 40 nM, where F_{585} and F_{651} are the fluorescence intensity at 585 nm and 651 nm in the absence or presence of Al^{3+}, respectively. Further application in Al^{3+}-spiked water samples suggested a recovery between 95 and 108%. The fluorescence response is highly selective for Al^{3+} over other metal ions with the addition of thiourea as the masking agent.

1. Introduction

The development of novel assays for environmentally and biologically important species, such as some metal ions, has been an important goal in the field of analytical chemistry.[1–3] Current approaches to detect these species include inductively coupled plasma mass spectrometry,[4] atomic absorption spectrometry,[5] and stripping voltammetry.[6] Although these methods offer excellent sensitivity and multi-element analysis, they are rather costly, time-consuming, complex, and non-portable. Fluorescent assays have the advantages of high sensitivity, specificity, and real-time monitoring with fast response time.[7,8] During the past few decades, a number of fluorescent assays were developed and have been used with some success in biological applications.[9–12] However, most of them display only one emission intensity change, although large fluorescence enhancement or efficient quenching is observed, as a sensing signal that responds to the concentration of the target. However, a fluorescence signal is readily disturbed by many factors, such as photobleaching, the concentration of fluorophore, stability illumination, sample environment (pH, solvent polarity and temperature, and so forth) and sensitivity of an instrument.[13–15] Therefore, single-emission detection is sometimes problematic for precise fluorometric analyses under biological conditions. Dual-signaling fluorescent (DSF) assays, which allow the measurement of two different emissions bands, are more attractive because the signal ratio between the two emission intensities can provide a built-in correction for the above-mentioned adverse effects on the fluorescence signals.[16,17]

Several principles have been exploited to design DSF assays. One of the most representative mechanisms is the combination of two signaling mechanisms, for example, conformational restriction and induction of charge transfer or internal charge transfer,[16] intermolecular excited state proton transfer,[18] photo-induced electron transfer and intramolecular charge transfer,[19] and excimer formation.[20] Recently, He and co-workers designed a dual-emission ratiometric fluorescent Cd^{2+} sensor based on the inhibition of resonance and charge delocalization.[21] The second mechanism is the binding-induced modulation of fluorescence resonance energy transfer (FRET).[22,23] The third regular mechanism is the nanosensor, which contains a reference fluorescence dye and a response fluorescence dye.[24–27] Most of the reported DSF assays have intrinsic challenges such as covalent linking between the receptor and the fluorophore, the poor solubility in

Henan Key Laboratory Cultivation Base of Nanobiological Analytical Chemistry, College of Chemistry and Chemical Engineering, Shangqiu Normal University, Shangqiu 476000, China. E-mail: xumaotian@sqnc.edu.cn; Fax: +86-370-2594306; Tel: +86-370-2595593

† Electronic supplementary information (ESI) available. See DOI: 10.1039/c1an15566k

water which results in having to be performed in an organic medium. More importantly, most the DSF assays exhibit fluorescence enhancement of one emission intensity at the expense of the other emission intensity.

To meet these challenges, dual-signaling fluorescence-enhancement (DSFE) assays, which are performed with a new working mechanism, are of great value. Therefore, we report here a novel strategy for designing DSFE assays based on the IFE, *i.e.* teh absorption of light at the excitation and/or emission wavelengths by absorbers in the detection system. The IFE can be a problem for any fluorescence measurement, especially where an absorbing component is being titrated into the cuvette, which results from the absorption of the excitation and/or emission light by absorbers in the detection system.[28–30] Although the IFE is usually considered as an annoying source of error in spectrofluorometry and should be avoided, recent studies have demonstrated its application in developing new fluorescent assays which do not require the establishing of any covalent linking between the receptor and the fluorophore.[31–33] However, no attempt, so far, has been made to design DSFE assays based on the IFE. Our proposed approach contains two structural motifs. One is the colorimetric and fluorometric enhancement dual-modal (DM) absorber. It is different from the common IFE-based fluorescent assays which work on the dark absorber. The other is a fluorophore which not only exhibits an excellent excitation or emission spectrum overlapping with the absorption maximum of the DM absorber or the DM absorber–target ensemble, but also the fluorescence emission of the fluorophore is not obviously affected by the target. To verify the novel strategy, herein, we describe a proof-of-concept example of a DSFE sensing system and a fluorescent ratiometric Al^{3+} assay functioning through this novel working mechanism. To demonstrate the feasibility of this design, Alizarin red S (ARS, Fig. 1A) and *meso*-tetra(*N*-methyl-4-pyridyl)porphine tetratosylate salt (TMPyP, Fig. 1B) were selected as the DM absorber and fluorophore, respectively. The suggested recognition mechanism of Al^{3+} by ARS was shown in Fig. 1C according to the published work.[34]

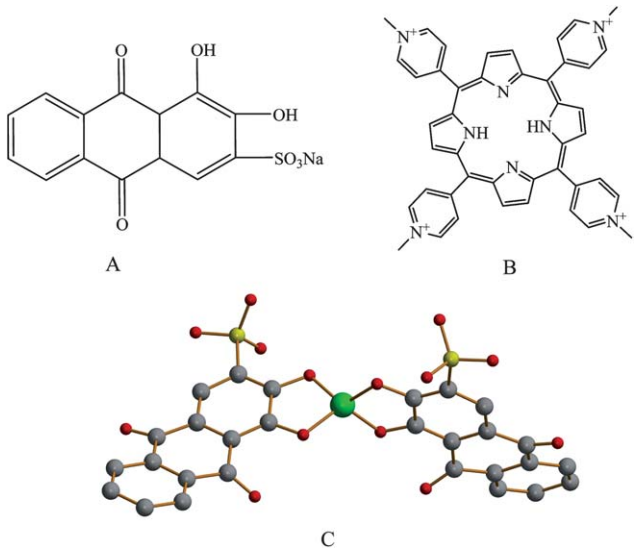

Fig. 1 Structures of ARS (A) and TMPyP (B) and recognition scheme of Al^{3+} by ARS (C).

2. Experimental

2.1. Materials and apparatus

TMPyP was purchased from Adrich-Sigma (USA). ARS, $AlCl_3$, sodium acetate (NaAc), acetic acid (HAc) and other salts used in this work were provided by China National Medicines Co. Ltd. (Shanghai, China). Stock solutions of $AlCl_3$ (0.1 M) were prepared by dissolving the desired amount of the material in Milli-Q ultrapure water (18.2 MΩ) and working solutions were obtained by serial dilution of the stock solutions with 0.2 M HAc–NaAc buffer solution (pH 5.5).

The UV-visible absorption spectra were recorded on a Hitachi U-4100 UV-vis spectrophotometer (Kyoto, Japan). All fluorescence measurements were performed on an RF-5301 fluorescence spectrophotometer (Shimadzu, Japan). Fluorescence emission spectra were collected after the addition of the desired materials (Al^{3+} or interference ions) using a bandwidth of 10 nm and a regular quartz cell containing 2.5 mL of solution. The pH was measured using a model 868 pH meter (Orion). All experiments were performed at room temperature.

2.2. Fluorometric titration of Al^{3+} using TMPyP

To test the effect of Al^{3+} on the fluorescence of TMPyP, fluorometric titration was done by adding a few microliters of a working solution of Al^{3+} to 2.5 mL 0.2 M HAc–NaAc (pH 5.5) buffer solution containing 0.1 μM TMPyP with a quartz cell (1.0 cm × 1.0 cm cross-section). The fluorescence emission spectra were obtained by excitation at 420 nm.

2.3. Performance of Al^{3+} detection

For Al^{3+} detection, 0.1 μM TMPyP, 2.0 μM ARS, and a proper amount of Al^{3+} (Table 1) or interfering metal ions solution were mixed and diluted to 2.5 mL with 0.2 M HAc–NaAc buffer solution (pH 5.5). After vigorous stirring for 1 min and allowing to stand for ~30 min at room temperature, the UV-vis absorption and fluorescence emission spectra were then recorded immediately.

3. Results and discussion

3.1. Assay mechanism

The signaling transduction scheme of our proposed assay is shown in Fig. 2A. ARS, an old and very cheap reagent, is a derivative of anthraquinone and a well-known biological staining agent. Since ARS is a metallochromic indicator which bears two hydroxyl groups and a sulfo group, it is used for spectrophotometric and titrimetric determinations.[35–37] First we explored the spectroscopic characteristics of ARS and the effect of Al^{3+} on the UV-vis and fluorescence spectra. In the absence of Al^{3+}, the absorption spectrum of ARS has a strong peak at 420 nm (curve 'a' in Fig. 2B), significantly overlapping with the excitation of TMPyP (curve 'b' in Fig. 2B). ARS ($\lambda_{abs} = 420$ nm) is expected to be capable of functioning as a powerful absorber to tune the emission of the fluorescence of TMPyP ($\lambda_{ex} = 420$ nm) on account of the spectral overlap. Thus, at high concentration of ARS, some of the TMPyP excitation will be filtered out, which controls the amount of light available to excite the fluorophore.

Table 1 Recovery data for the determination of Al^{3+} in Al^{3+}-spiked tap water and lake water by our assay

Samples	Al^{3+} added (100 nM)	Al^{3+} detected (100 nM)	Recovery (%)	RSD (%)
Tap water	5	5.06	103	2.4
	10	10.3	108	2.7
Chunyun Lake water	5	5.11	97	2.5
	10	9.82	102	2.6
Nanhu Lake water	5	4.86	95	2.8
	10	10.1	101	3.0

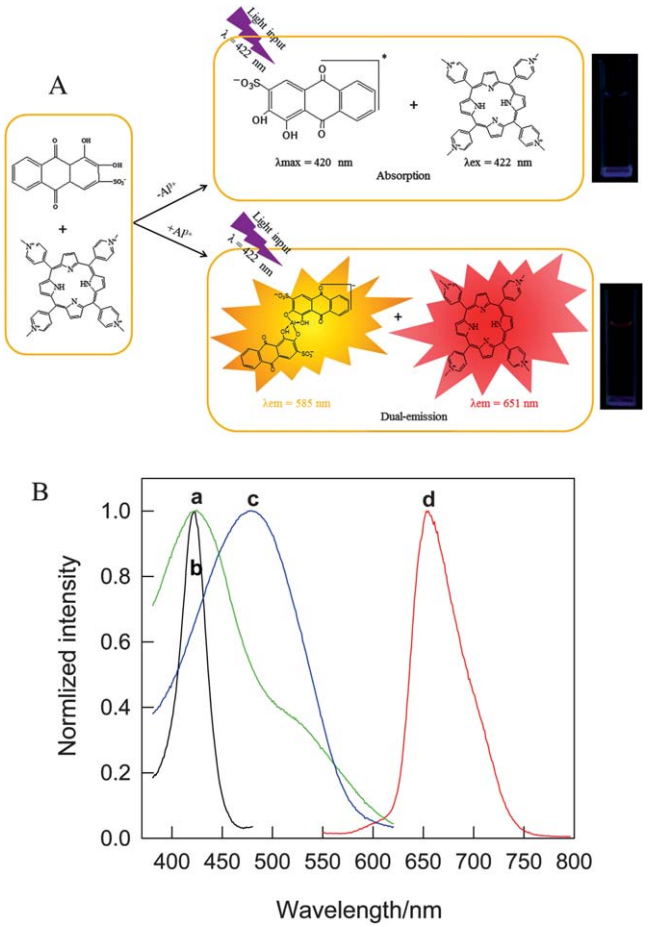

Fig. 2 (A) Scheme of the mechanism of the proposed assay. (B) Absorption spectrum of ARS in the absence of Al^{3+} (a), fluorescence excitation spectrum of TMPyP ($\lambda_{ex} = 422$ nm) (b), absorption spectrum of ARS in the presence of 10 μM Al^{3+} (c), and emission spectrum of TMPyP ($\lambda_{em} = 651$ nm) (d) in HAc–NaAc buffer solution (pH 5.5, 0.2 M).

However, in the presence of Al^{3+}, the absorption spectrum of the ARS/Al^{3+} complex has a strong peak at 480 nm (curve 'c' in Fig. 2B), which overlaps negligibly with the excitation band of TMPyP and leads to more light being available to excite the fluorophore and turn-on the proper emission spectrum for TMPyP (curve 'd' in Fig. 2B).

After characterization of the IFE, fluorescence studies were carried out to investigate the interaction of Al^{3+} with ARS using UV-vis and fluorescence spectroscopy. The UV-vis response of ARS to Al^{3+} shows an obvious concentration-dependent red-shift of the maximum absorption peak from 420 nm to 480 nm (Fig. S1 in the supporting information†). As indicated in Fig. 3, the fluorescence spectrum of ARS in HAc–NaAc buffer solution is sensitive to Al^{3+} and increased with the increasing amount of Al^{3+}, suggesting that Al^{3+} most likely forms the stable fluorescent complex with the ARS. Upon the addition of Al^{3+} (from 0 to 20 μM) a significant increase in 585 nm was observed. Once the concentration of Al^{3+} is over 30 μM, the fluorescence intensity reaches a plateau, suggesting the saturation of the recognition sites by Al^{3+} binding – see the inset of Fig. 3.

Compared with the known DSFE sensing system for fluorescent ratiometric Al^{3+} assay reported in the literature,[20,38] the present design possesses at least four remarkable features. First, one could successfully avoid the covalent linking between the receptor and the fluorophore, which offers considerable flexibility in the design and more simplicity. Second, the novel DSFE sensing system can work in pure aqueous solutions. Third, the new fluorescent ratiometric Al^{3+} assay shows a large Stoke's shift (the maximum shift is 230 nm). Most classical fluorescent sensors have the fatal disadvantage that their Stoke's shifts are small. A small Stoke's shift can cause self-quenching and measurement

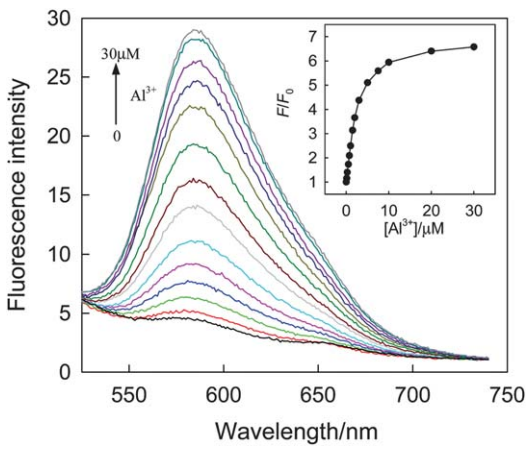

Fig. 3 Fluorescence emission spectra of ARS (2 μM) in the presence of different concentrations of Al^{3+} varying from 0, 0.1, 0.25, 0.5, 0.75, 1, 1.5, 2, 3, 5, 7.5, 10, 20, 30 μM in HAc–NaAc buffer solution. The arrow indicates the fluorescence enhancement as the Al^{3+} ion concentration is increased. Spectra were acquired with excitation at 420 nm at room temperature. Inset: ratio of fluorescence intensities (F_{585}/F_0) as a function of Al^{3+}concentration, where F_{585} and F_0 represent the fluorescence intensity at 585 nm in the presence and absence of Al^{3+}, respectively.

error by excitation light and scattered light.[39–41] Lastly, the proposed sensing approach presented here seems to be universal and can be applied to any DM dye-based assays by selecting a suitable fluorophore.

3.2. Effect of Al^{3+} on fluorescence emission of TMPyP

For evaluation of validity of the proposed principle, the effect of different concentrations of Al^{3+} on the fluorescence emission of TMPyP was investigated in HAc–NaAc buffer solution. Fig. S2† in the supporting information shows that the fluorescence spectra of TMPyP were almost identical in both the absence and the presence of Al^{3+} up to 1 mM.

3.3. ARS-induced quenching of the fluorescence emission of TMPyP

As observed in Fig. S3† in the supporting information, the fluorescence intensity of TMPyP in HAc–NaAc buffer solution decreased obviously upon the addition of the increasing amount of ARS. In the absence of ARS, TMPyP exhibits an intense emission at 651 nm. In the presence of ARS, the mixture of ARS (4 μM) and TMPyP (0.1 μM) is weakly emissive. There are only minimal changes in the presence of ARS from 4 μM to 10 μM. At ARS concentrations more than 10 μM, no further decrease in fluorescence is observed and a plateau is reached, as shown in inset of Fig. S3.† These data indicate that ARS is a good candidate to modulate the fluorescence of TMPyP based on the IFE, as expected.

3.4. Assay optimization

The molar ratio of the non-covalent ARS/TMPyP ensemble was found to strongly affect the fluorescence response toward Al^{3+}. The molar ratio was optimized first to enhance the performance of the assay by fixing TMPyP at 0.1 μM and varying the ARS concentrations. As shown in Fig. 4, the dual-signal fluorescence enhancement (F_{585}/F_{651}) response of the ARS/TMPyP complex to Al^{3+} for three composition ratios was plotted as a function of the concentration of Al^{3+} in HAc–NaAc buffer solution, where F_{651} and F_{585} are the fluorescence intensities at 651 nm and 585 nm with increasing amounts of Al^{3+}. Obviously, depending on the molar ratio of the fluorophore and DM absorber, there are different response characteristics (linear dynamic range and response sensitivity) of the proposed DSFE sensing system. A higher concentration of ARS would quench the fluorescence almost completely and decrease the blank fluorescence signal value, which will increase the dynamic working range of the measurement. However, the amount of ARS in the system should not be too high because the response sensitivity is significantly smaller than that obtained using a lower concentration of ARS. On the other hand, lower concentrations of ARS result in the higher blank fluorescence intensity of the assay. Thus, it decreases the sensitivity and response range of the measurement. Therefore, as shown in Fig. 4, the present experiment showed the best response in terms of both the sensitivity and linear dynamic range when the molar ratio of ARS to TMPyP is 20 : 1, compared with that obtained when the molar ratio is 10 : 1 and 30 : 1, respectively.

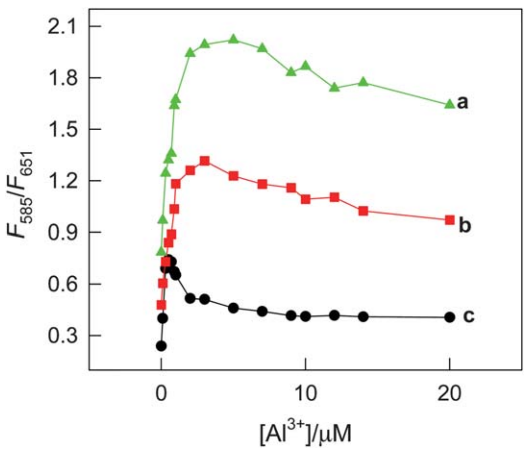

Fig. 4 Fluorescence response to Al^{3+} in the presence of different molar ratios of ARS and TMPyP (fixing at 0.1 μM). The molar ratios of ARS and TMPyP were 30 : 1 (a), 20 : 1 (b), and 10 : 1 (c), respectively. The curve was plotted with the fluorescence intensity ratio (F_{585}/F_{651}) *vs.* different Al^{3+} concentrations (0, 0.1, 0.3, 0.5, 0.7, 0.9, 1, 1.5, 2, 3, 5, 7, 9, 10, 12, 14, 20, 30, 40 and 50 μM). F_{585} and F_{651} represent the fluorescence intensity at 585 nm or 651 nm in the presence different concentrations of Al^{3+}, respectively.

Having arrived at the optimal composition ratio of the ARS and TMPyP, we then investigated the effect of acidity of the solution on the fluorescence response to Al^{3+} because the pH value of the environment around the fluorescent probe for metal ions usually shows somewhat of an effect on its performance because of the protonation or deprotonation reaction for the ARS/TMPyP or the hydrolysis reaction for the metal ions in the alkaline conditions.[32] To examine the effect of pH, titration experiments were carried out using HAc–NaAc buffer solution with different pH. Fig. S4† in the supporting information depicts the pH dependence of the fluorescence intensity enhancement of the ARS/TMPyP complex by Al^{3+}. The fluorescence intensity ratio of the system, F_{585}/F_0, increased with increasing pH and reached a plateau when the pH is above 5.0, where F_{585} and F_0 represent the fluorescence intensities at 585 nm in the presence or absence of Al^{3+}, respectively. It is obvious that F_{585}/F_0 is independent of pH in the range of 5.0–5.8. In our experiment, we chose HAc–NaAc (pH 5.5) buffer solution as the optimal buffer system.

3.5. Selectivity

Next we investigated the selectivity of our assay for Al^{3+} over other metal ions including common environmentally or biological relevant metal ions such as Mg^{2+}, Ca^{2+}, Cd^{2+}, Co^{2+}, Pb^{2+}, Mn^{2+}, Cu^{2+}, Fe^{3+}, Hg^{2+} and Zn^{2+}. Solutions containing these metal ions were then tested under the same conditions to evaluate the selectivity of our DSFE Al^{3+} assays. As shown in Fig. 5, our assay was highly selective for Al^{3+} over the other metal ions we tested in the presence of thiourea as the masking agent. The fluorescence at both 651 nm and 585 nm was slightly affected by the metal ions we tested other than Al^{3+} from 0 to 50 μM. In particular, only the Al^{3+} can enhance the fluorescence at 585 nm significantly, as can be seen in Fig. S5† in the supporting information. And then we detected Al^{3+} in the absence and the presence of the mixture of the metal ions (5 μM). The fluorescence

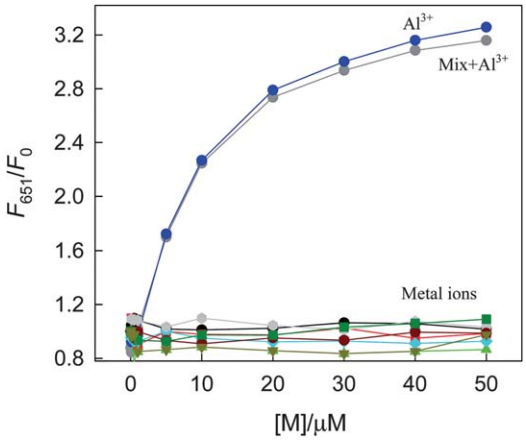

Fig. 5 Fluorescence enhancement (F_{651}/F_0) response of ARS/TMPyP complex to different metal ions (Al^{3+}, Mg^{2+}, Ca^{2+}, Cd^{2+}, Co^{2+}, Pb^{2+}, Mn^{2+}, Cu^{2+}, Fe^{3+}, Hg^{2+} and Zn^{2+} separately) and the mixed metal ions with increasing concentrations of metal ions at 0, 0.1, 0.5, 1, 5, 10, 20, 30, 40 and 50 μM in HAc–NaAc buffer solution. F_{651} and F_0 represent the fluorescence intensity at 651 nm in the presence or absence different concentrations of metal ions, respectively. The excitation was 422 nm, and emission was recorded at 651 nm.

response to Al^{3+} showed no obvious difference in the absence and presence of the mixture of the metal ions. These results suggest that the metal ions we tested should not interfere with the assay of Al^{3+} when applying our proposed assay in practice.

3.6. Sensitivity

Taken together, these findings demonstrate that the present DSFE sensing system could be an alternative approach for use in fluorescent ratiometric Al^{3+} assays. We thus successively evaluated the working ability of the method for Al^{3+} detection. Under the optimal conditions, when a certain amount of Al^{3+} was added, the proposed assay gave two signals at 585 nm and 651 nm corresponding to the emission of the ARS/Al^{3+} complex and TMPyP, respectively. Fig. 6A displays the typical fluorescence spectra as functions of the different amounts of Al^{3+} from 0.1 to 50 μM. Upon the addition of an increasing amount of Al^{3+}, there is a gradual increase in dual-signal fluorescence. To quantify concentrations of Al^{3+} based on the increment in the dual-signal fluorescence, we measured the saturated fluorescence upon the addition of different concentrations of Al^{3+}. When the concentration of Al^{3+} was over 50 μM, the dual-emission showed almost no further change (data not shown). Moreover, colorimetric assays were utilized to monitor the fluorescent color changes for different Al^{3+} concentrations. As shown in Fig. 6B, a fluorescence color change from colorless to red upon UV irradiation using a commercially available UV lamp ($\lambda = 365$ nm) was observed by the naked eye upon the addition of Al^{3+} to the ARS/TMPyP complex. These results indicated that the visual detection of Al^{3+} just by the color change observed by the naked eye is successful.

Fig. 7 shows the region between 0.1 and 1.5 μM Al^{3+} where a linear relationship ($F = 0.502C + 0.570$, $R^2 = 0.992$) was observed between Al^{3+} concentration and the ratio of the dual-signal fluorescence (F_{585}/F_{651}). The limit of detection that is

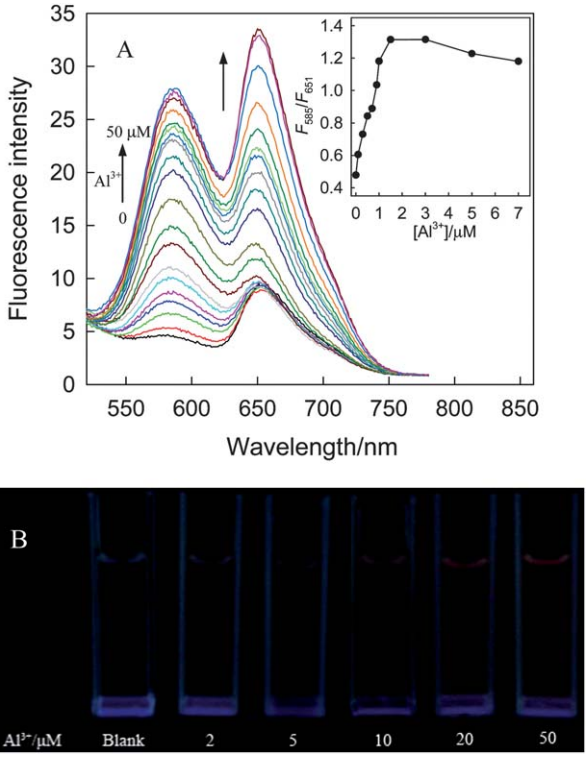

Fig. 6 (A) Fluorescence spectra of TMPyP/ARS complex upon the addition of Al^{3+} (0, 0.1, 0.3, 0.5, 0.7, 0.9, 1, 1.5, 2, 3, 5, 7, 9, 10, 12, 14, 20, 30, 40 and 50 μM) in HAc–NaAc buffer solution. The arrows indicate the dual-signal fluorescence enhancement as increase Al^{3+} concentrations. Spectra were acquired with excitation at 420 nm. Inset: fluorescent ratio (F_{585}/F_{651}) as a function of Al^{3+} concentration, where F_{585} and F_{651} represent the fluorescence intensity at 585 nm or 651 nm in the presence of different concentrations of Al^{3+}, respectively. (B) Photographs of the proposed sensor upon the addition of different amounts of Al^{3+} under UV irradiation (365 nm). The photos were taken using a commercially available UV lamp.

taken to be 3 times the standard deviation in blank solution was calculated to be 40 nM, which is comparable with other Al^{3+} fluorescent assays (or lower than similar assays).[9,20,38] And the

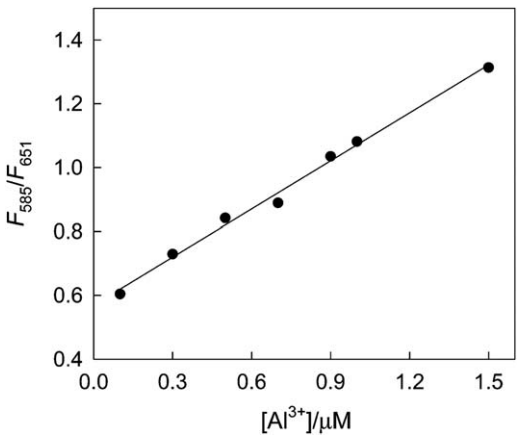

Fig. 7 The linear relation between the fluorescent ratio (F_{585}/F_{651}) and the concentration of Al^{3+}, where F_{585} and F_{651} represent the fluorescence intensity at 585 nm or 651 nm in the presence of different concentrations of Al^{3+}, respectively.

performance of some optical Al^{3+} sensors is summarized in Table S1† in the supporting information.

3.7. Fluorescence assay for Al^{3+} in water samples

To further investigate the practicality of the proposed method, we applied a standard addition method to detect Al^{3+} in both tap and lake water samples. For tap water, the sample was collected after discharging tap water for 20 min and boiling for 5 min to remove chlorine. Lake water samples were obtained from Chunyun Lake on the campus of Shangqiu Normal University and Nanhu Lake in Nanhu Park. The samples collected were first filtered through a column (packed with an anionic-exchange resin) to remove oils and other organic impurities. All the water samples were spiked with standard Al^{3+} solution at different concentration levels, which were prepared on the basis of possible metal ions presenting in the environmental water and then analyzed with the method proposed. The results showed a recovery between 95 and 108% (as shown in Table 1), which indicated the accuracy and reliability of the present method for Al^{3+} determination in practical applications.

4. Conclusion

We have presented a new strategy for designing DSFE assays. We developed a sensitive and selective fluorescent ratiometric Al^{3+} assay, as an example, working through this novel strategy in aqueous media based on the IFE between a DM absorber (ARS) and fluorophore (TMPyP). The success of the fluorescent ratiometric detection of Al^{3+} based on the IFE between ARS and TMPyP unquestionably demonstrates that the feasibility of our proposed strategy for designing DSFE assays could be easily achieved by using some other DM absorber and fluorophore. The present study provides a novel strategy to design a DSFE assay without the need for covalent linking between the receptor and signaling unit and has the good water solubility. These features establish the simplicity, affectiveness and universality of the strategy and could, therefore, provide the groundwork for the design of DSFE assays for applications.

Acknowledgements

The work was supported by the National Natural Science Foundation of China (21105063, 21175091).

References

1 R. H. Newman, M. D. Fosbrink and J. Zhang, *Chem. Rev.*, 2011, **111**, 3614–3666.
2 J. F. Zhang, Y. Zhou, J. Yoon and J. S. Kim, *Chem. Soc. Rev.*, 2011, **40**, 3416–3429.
3 J. Wu, W. Liu, J. Ge, H. Zhang and P. Wang, *Chem. Soc. Rev.*, 2011, **40**, 3483–3495.
4 B. Chen, Y. Zeng and B. Hu, *Talanta*, 2010, **81**, 180–186.
5 C. G. Magalhães, K. L. A. Lelis, C. A. Rocha and J. B. B. d. Silva, *Anal. Chim. Acta*, 2002, **464**, 323–330.
6 Q. Li, L. Wang, D. Xi and G. Lu, *Food Chem.*, 2006, **97**, 176–180.
7 J. R. Lakowicz, *Principles of Fluorescence Spectroscopy*, Springer, New York, 3rd edn, 2006.
8 A. M. Powe, S. Das, M. Lowry, B. El-Zahab, S. O. Fakayode, M. L. Geng, G. A. Baker, L. Wang, M. E. McCarroll, G. Patonay, M. Li, M. Aljarrah, S. Neal and I. M. Warner, *Anal. Chem.*, 2010, **82**, 4865–4894.
9 (*a*) D. Maity and T. Govindaraju, *Inorg. Chem.*, 2010, **49**, 7229–7231; (*b*) D. Maity and T. Govindaraju, *Chem. Commun.*, 2010, **46**, 4499–4501; (*c*) S. C. Warren-Smith, S. Heng, H. Ebendorff-Heidepriem, A. D. Abell and T. M. Monro, *Langmuir*, 2011, **27**, 5680–5685.
10 Y. Liu, C. Deng, L. Tang, A. Qin, R. Hu, J. Z. Sun and B. Z. Tang, *J. Am. Chem. Soc.*, 2011, **133**, 660–663.
11 Y. Kurishita, T. Kohira, A. Ojida and I. Hamachi, *J. Am. Chem. Soc.*, 2010, **132**, 13290–13299.
12 Z. Xu, K.-H. Baek, H. N. Kim, J. Cui, X. Qian, D. R. Spring and J. Y. I. Shin, *J. Am. Chem. Soc.*, 2010, **132**, 601–610.
13 M. D. Yilmaz, S. H. Hsu, D. N. Reinhoudt, A. H. Velders and J. Huskens, *Angew. Chem., Int. Ed.*, 2010, **49**, 5938–5941.
14 T. Ogawa, J. Yuasa and T. Kawai, *Angew. Chem., Int. Ed.*, 2010, **49**, 5110–5114.
15 H. Peng, J. A. Stolwijk, L. Sun, J. Wegener and O. S. Wolfbeis, *Angew. Chem., Int. Ed.*, 2010, **49**, 4246–4249.
16 J. V. Mello and N. S. Finney, *Angew. Chem., Int. Ed.*, 2001, **40**, 1536–1538.
17 Y.-H. Chan, C. Wu, F. Ye, Y. Jin, P. B. Smith and D. T. Chiu, *Anal. Chem.*, 2011, **83**, 1448–1455.
18 K. Choi and A. D. Hamilton, *Angew. Chem., Int. Ed.*, 2001, **40**, 3912–3915.
19 M. Yuan, Y. Li, J. Li, C. Li, X. Liu, J. Lv, J. Xu, H. Liu, S. Wang and D. Zhu, *Org. Lett.*, 2007, **9**, 2313–2316.
20 W. Lin, L. Yuan and J. Feng, *Eur. J. Org. Chem.*, 2008, **2008**, 3821–3825.
21 L. Xue, G. Li, Q. Liu, H. Wang, C. Liu, X. Ding, S. He and H. Jiang, *Inorg. Chem.*, 2011, **50**, 3680–3690.
22 Z. Han, X. Zhang, Z. Li, Y. Gong, X. Wu, Z. Jin, C. He, L. Jian, J. Zhang, G. Shen and R. Yu, *Anal. Chem.*, 2010, **82**, 3108–3113.
23 L. Long, W. Lin, B. Chen, W. Gao and L. Yuan, *Chem. Commun.*, 2011, **47**, 893–895.
24 C. Zong, K. Ai, G. Zhang, H. Li and L. Lu, *Anal. Chem.*, 2011, **83**, 3126–3132.
25 E. J. Park, M. Brasuel, C. Behrend, M. A. Philbert and R. Kopelman, *Anal. Chem.*, 2003, **75**, 3784–3791.
26 H. A. Clark, R. Kopelman, R. Tjalkens and M. A. Philbert, *Anal. Chem.*, 1999, **71**, 4837–4843.
27 H. A. Clark, M. Hoyer, M. A. Philbert and R. Kopelman, *Anal. Chem.*, 1999, **71**, 4831–4836.
28 B. Fanget and O. Devos, *Anal. Chem.*, 2003, **75**, 2790–2795.
29 G. Gabor and D. R. Walt, *Anal. Chem.*, 1991, **63**, 793–796.
30 H. He, H. Li, G. Mohr, B. Kovacs, T. Werner and O. S. Wolfbeis, *Anal. Chem.*, 1993, **65**, 123–127.
31 N. Shao, Y. Zhang, S. Cheung, R. Yang, W. Chan, T. Mo, K. Li and F. Liu, *Anal. Chem.*, 2005, **77**, 7294–7303.
32 L. Shang and S. Dong, *Anal. Chem.*, 2009, **81**, 1465–1470.
33 (*a*) L. Shang, C. Qin, L. Jin, L. Wang and S. Dong, *Analyst*, 2009, **134**, 1477–1482; (*b*) Y. Zhai, L. Jin, P. Wang and S. Dong, *Chem. Commun.*, 2011, **47**, 8268–8270.
34 R. Saisathish, M. Ravikumar, G. Nageswararao, K. Anilkumar and C. Janardhana, *Spectrochim. Acta, Part A*, 2007, **66**, 457–461.
35 V. M. Ivanov, E. M. Adamova and V. N. Figurovskaya, *J. Anal. Chem.*, 2010, **65**, 473–481.
36 R. Villamil-Ramos and A. K. Yatsimirsky, *Chem. Commun.*, 2011, **47**, 2694–2696.
37 L. Zhang, S. Dong and L. Zhu, *Chem. Commun.*, 2007, 1891–1893.
38 T. Ma, M. Dong, Y. Dong, Y. Wang and Y. Peng, *Chem.–Eur. J.*, 2010, **16**, 10313–10318.
39 U. C. Saha, B. Chattopadhyay, K. Dhara, S. K. Mandal, S. Sarkar, A. R. Khuda-Bukhsh, M. Mukherjee, M. Helliwell and P. Chattopadhyay, *Inorg. Chem.*, 2011, **50**, 1213–1219.
40 F. Wang, R. Nandhakumar, J. H. Moon, K. M. Kim, J. Y. Lee and J. Yoon, *Inorg. Chem.*, 2011, **50**, 2240–2245.
41 L. Yuan, W. Lin, Y. Yang and J. Song, *Chem. Commun.*, 2011, **47**, 4703–4705.

